Heliyon 6 (2020) e05546

Contents lists available at ScienceDirect

Heliyon

journal homepage: www.cell.com/heliyon

Research article

Casuarictin: A new herbal drug molecule for Alzheimer's disease as inhibitor of presenilin stabilization factor like protein

Rupali Kumari, Amit Chaudhary, Ashutosh Mani *

Department of Biotechnology, Motilal Nehru National Institute of Technology Allahabad, Prayagraj 211004, India

ARTICLE INFO

Keywords:
Neuroscience
Cell biology
Bioinformatics
Proteins
Pharmaceutical science
Molecular biology
PSFL
Presenilin
Casuarictin virtual screening
Docking
Molecular dynamics simulation

ABSTRACT

Alzheimer's disease is a progressive neurodegenerative disorder. In this disease neurodegeneration occurs due to deposition of aggregated amyloid-beta plaques and neurofibrillary tangles (hyperphosphorylated tau proteins). Present study focuses on interaction of different phytochemicals with presenilin stabilization factor like protein (PSFL). PSFL protein is known to stabilize Presenilin, which is mainly involved in intramembrane hydrolysis of selected type- I membrane proteins, including amyloid-beta precursor protein, and produces amyloid-beta protein. Amyloid-beta are small peptides comprising of 36–43 amino acids, which play a significant role in senile plaques formation in the brains of Alzheimer patients. Virtual screening and docking of phytochemicals with PSFL protein was done to find the potential inhibitor. Based on binding affinity, docked energy and molecular dynamics simulations, three phytochemicals namely Saponin, Casuarictin, and Enoxolone, were identified as potential inhibitors for the target protein.

1. Introduction

Alois Alzheimer discovered Alzheimer's disease in 1906. He observed many abnormal clumps (amyloid plaques) and tangled bundles of fibers (neurofibrillary, or tau tangles) in the brain tissue of a woman who had died of an unusual mental illness [1, 2]. Symptoms included language problems, memory loss, and abnormal behaviour, which play an essential role in AD [3, 4, 5]. AD is a progressive neurodegenerative disorder that usually occurs in the older people [6]. In this disease, neuronal death takes place due to deposition of aggregated amyloid-beta plaques and neurofibrillary tangles (hyperphosphorylated tau) in the brain [7, 8, 9]. Rapid production of amyloid-beta takes place due to alteration in proteolysis of amyloid precursor protein (APP) caused by missense mutations in amyloid precursor protein (APP), PS-1 (presenilin-1), and PS-2 (presenilin-2) [10]. This causes release of cytokines and activation of microglia as inflammatory responses due to the accumulation of amyloid-beta plaques. Also, hyperphosphorylation of tau protein takes place due to disturbance in equilibrium between kinases and phosphatases [11, 12].

Recently, PSFL, which plays key role in stabilizing presenilin protein, has been found to be crucial in Alzheimer's disease [13, 14]. Presenilins are proteins mainly involved in intramembrane hydrolysis of selected type- I membrane proteins. Pertinently amyloid-beta precursor protein (APP) are also type- I membrane proteins that are cleaved by BACE-1 enzyme to produce Amyloid beta (Aβ) peptides. Amyloid beta (Aβ) are small peptides comprising of 36–43 amino acids, which play a crucial role in senile plaques formation. It is found in the brain of Alzheimer patients [15, 16]. Finding a potent drug that binds to PSFL protein and destabilizes Presenilins may help in treating Alzheimer's disease by reducing the formation of amyloid-beta protein.

Alzheimer's disease has no cure till now, but there are some drugs recently approved by the U.S. Food and Drug Administration (FDA) to treat the symptoms. Donepezil, galantamine, and rivastigmine are among available medications that act as cholinesterase inhibitors [3, 17]. These drugs inhibit the hydrolysis of a neurotransmitter, Acetylcholine in the brain, that is important for cognitive functioning, memory, and emotion. Tacrine was the first approved Acetylcholinesterase inhibitor, which was developed for the treatment of Alzheimer's disease, but it was toxic towards the liver [14]. So, Tacrine was withdrawn from the pharmaceutical market. Another drug, memantine, regulates the activity of different neurotransmitters in the brain. Also, a combination of the cholinesterase inhibitors (donepezil) with NMDA receptor antagonists (Memantine) is another medication used for treatment. Thus, treating Alzheimer's

* Corresponding author.
E-mail address: amani@mnnit.ac.in (A. Mani).

https://doi.org/10.1016/j.heliyon.2020.e05546
Received 21 June 2020; Received in revised form 12 October 2020; Accepted 16 November 2020

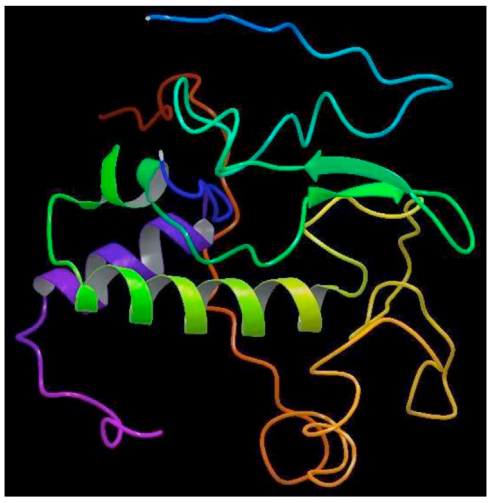

Figure 1. Three dimensional (3D) structure of PSFL protein predicted by Modeller.

disease at the molecular level will be more helpful than just treating the symptoms.

Alzheimer's disease may develop due to different factors such as Aging, a family history of Alzheimer's disease and presence of genes β-amyloid precursor protein (APP), apolipoprotein E (APOE), and presenilin 1 (PS-1) [18]. There are some factors that may increase the risk of Alzheimer's disease, such as undergoing severe or repeated traumatic brain injuries (TBI) and exposure to some environmental contaminants, such as pesticides, industrial chemicals and toxic metals [19, 20]. This study aims to model PSFL protein structure and identify a potent inhibitor for the treatment of AD. There are studies that have already used this technique to find out inhibitors against a target protein [21, 22, 23].

2. Materials and methods

2.1. Retrieval of the ligands from database

Natural Products (Herbal Ingredients Targets containing 802 ZINC entries) Ligands database were retrieved from the ZINC database in *.sdf* format, and some other phytochemicals such as carotenoids, flavonoids, polyphenols, terpenes also downloaded from the PubChem database. Some medicinal plants like Blueberry [24], Cannabidiol [25], Curcuma [26], and *Phyllanthus Emblica* [27] phytochemicals were also used as a ligand which has already been reported for treatment of AD. All these phytochemicals were further converted in PyRx 0.8, a supportable format by using Open Babel [28]. These all ligand databases were used for virtual screening.

2.2. Retrieval of target protein sequence

Presenilin stabilization factor-like protein [*Homo sapiens*] sequence was retrieved from NCBI having GenBank ID AAN63817.1 and sequence

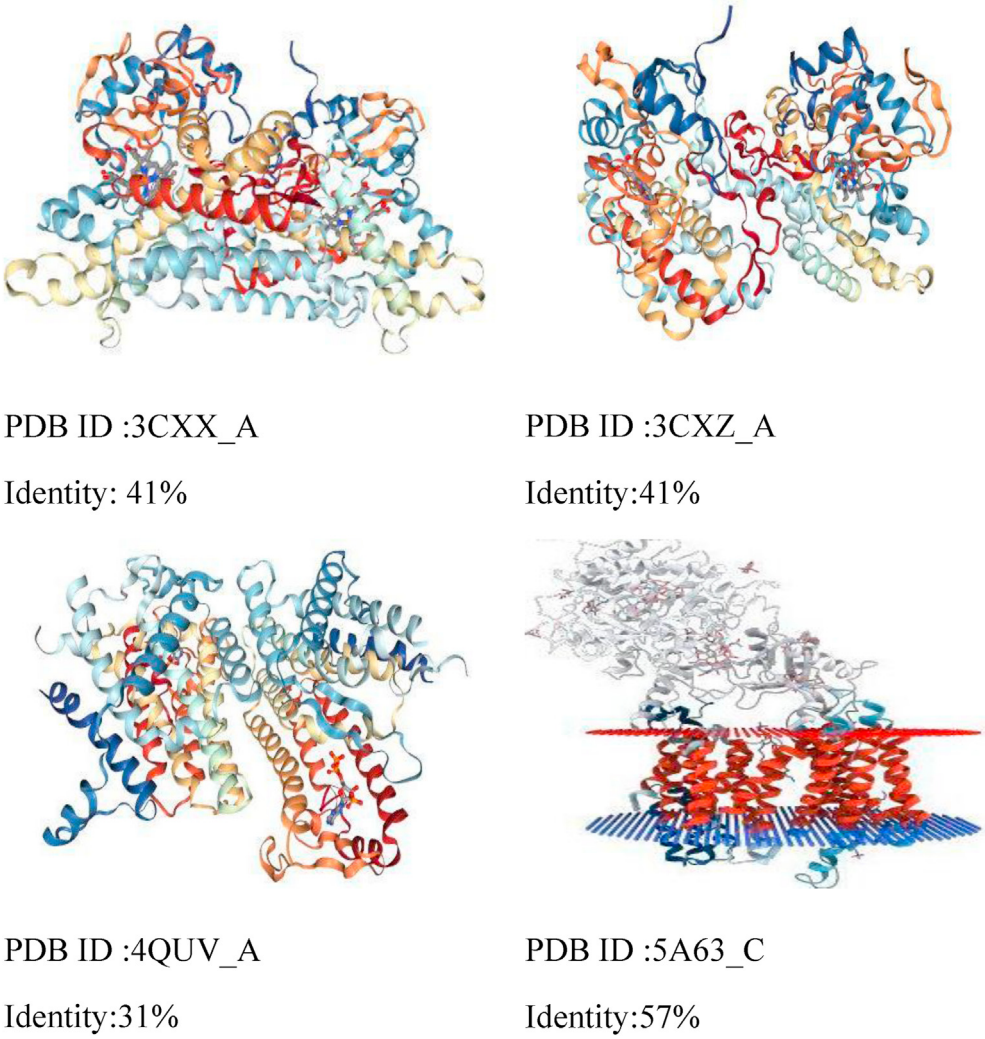

Figure 2. Four template sequences showing structure and identity with the PSFL protein.

Table 1. Ramachandran Plot statistics of the best model Seq.B99990002.

	Number of residues	%
Most favoured regions	138	84.7%
Additional allowed regions	18	11.0%
Generously allowed regions	4	2.5%
Disallowed regions	3	1.8%
Non-glycine and non-proline residues	163	100%
End-residues (excl. Gly and Pro)	2	
Glycine residues	18	
Proline residues	4	
Total number of residues	187	

Table 2. DOPE (Discrete Optimized Protein Energy) score of the generated models.

S.No.	Name of Models generated	DOPE Score
1.	Seq.B99990001	-14792.358398
2.	Seq.B99990002	-14559.158203
3.	Seq.B99990003	-14337.731445
4.	Seq.B99990004	-14080.270508
5.	Seq.B99990005	-15077.041016

length 257 amino acids [29], further it was used for tertiary structure prediction.

2.3. Structure prediction of target protein and their validation

Homology modeling was done to predict the three-dimensional structure of Presenilin stabilization factor-like protein by using Modeller 9.19 [30]. BLAST tool was used to predict homologous protein [31] [Figure 1]. The target protein was taken in FASTA format and four templates in PDB format for the modeling purpose. For template selection, PSI-BLAST of PSFL protein was done against the PDB database, and four templates (PDB ID: 3CXX_A, 3CXZ_A, 4QUV_A, and 5A63_C) were selected on the basis of sequence identity having >30 % [Figure 2]. At last, five homology models were generated and further validated through PDBsum generate by Ramachandran plot statistics [32] [Table 1]. Five homology models of PSFL protein were generated using Modeller. Their DOPE score has been given in Table 2.

2.4. Virtual screening of phytochemicals with modelled PSFL protein

Virtual screening (VS) is a computational approach used in drug discovery field to screen large databases or collections of compounds in order to identify novel hits [33]. Virtual screening was carried out by using PyRx 0.8, which follows the Autodock Vina program. All the phytochemicals were subjected to screening against the modelled protein.

2.5. Docking of screened ligands with modelled PSFL protein

Molecular docking is a popular approaches for studying binding affinity of ligand and protein [34]. Depending upon binding properties of ligand and target, it predicts the three-dimensional structure of the complexes.

Ten best scoring phytochemicals selected after virtual screening [Figure 3] were further used for molecular docking with modelled PSFL protein. AutoDock Tool 4.2 was used for docking which follows the Search Parameter, Genetic Algorithm, and simulated annealing [35].

2.6. Molecular dynamics simulation of top protein-ligand complex

The study about structure of macromolecules (Proteins, Nucleic acid, Peptides) is a key point for exploring important cellular processes. Molecular dynamics simulation (MDS) is another approach in the field of bioinformatics for the study of the atom location in space. Newton's laws of motion are used to calculate the surface energy of system. MD simulations was used to investigate information on the fluctuations and conformational changes of macromolecules [36, 37, 38]. After docking, GROMACS version 5.1.2 software was used to check the stability of PSFL protein. MD simulation was done for three top protein-ligand complexes [39]. Topologies for the complex were generated using AMBER03 force field [40]. Protons were automatically assigned to the protein-ligand complex using the program pdb2 gmx within the GROMACS package. TIP3P water model was used for the solvation of Complex systems in a triclinic box under the periodic boundary conditions using a distance of 1.2 nm from the protein to the surface of the box. Energy minimization of each system was done using the steepest descent integrator without constraints for 2000 steps [41]. After energy minimization, equilibration of systems was done under NVT (canonical ensemble) and NPT (isothermal–isobaric ensemble) conditions for 100 ps at 300 K after applying position restraints to the protein (Andersen HC et al., 1980). Finally, a 5000 ps production run was performed under NPT conditions by removing position restraints. Maintenance of temperature and pressure of the system was done using Berendsen weak-coupling method [39]. Lennard-Jones potential was used for van der Waals interactions, and electrostatic interactions were maintained using particle-mesh Ewald electrostatics calculations with a cut-off for the real space term of 0.8 nm [42]. All the bonds were constrained using the LINCS algorithm [43]. A 2 fs time step was applied, and at 2 ps final coordinates were saved. Analysis of MD simulation was done using Gromacs in-built tools such as root-mean-square deviation (RMSD), solvent-accessible surface area (SASA), root mean square fluctuation (RMSF) and radius of gyration (Rg). Rg calculation was done using least-squares fit [44]. The production simulation was performed for 20 ns at 300 K. For all trajectory analysis and graph plotting, Xmgrace tool was used [45]. Analysis of MD trajectories was done using gmx_rmsd, gmx_SASA, gmx_rmsf, and gmx_gyration of GROMACS utilities to get the best results.

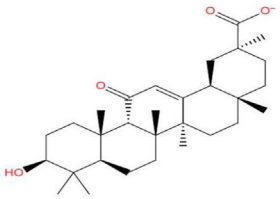

ZINC 38140512

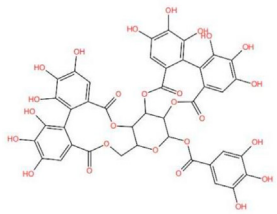

ZINC73644

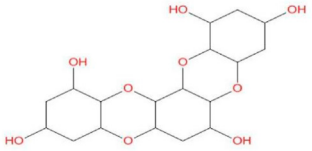

ZINC73162010

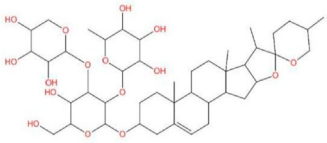

ZINC21630000

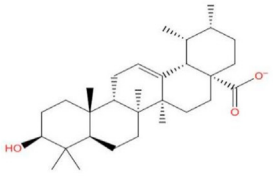

ZINC 03947455

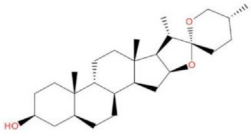

ZINC 08214878

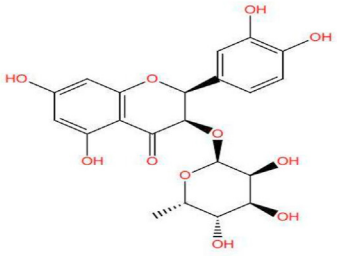

ZINC 05369368

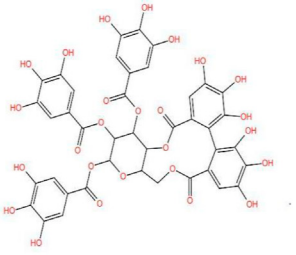

ZINC151590

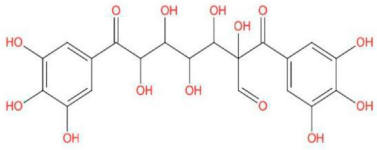

ZINC129650701

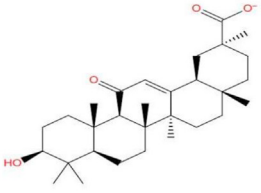

ZINC 19203131

Figure 3. Top 10 best phytochemicals with their structure IDs.

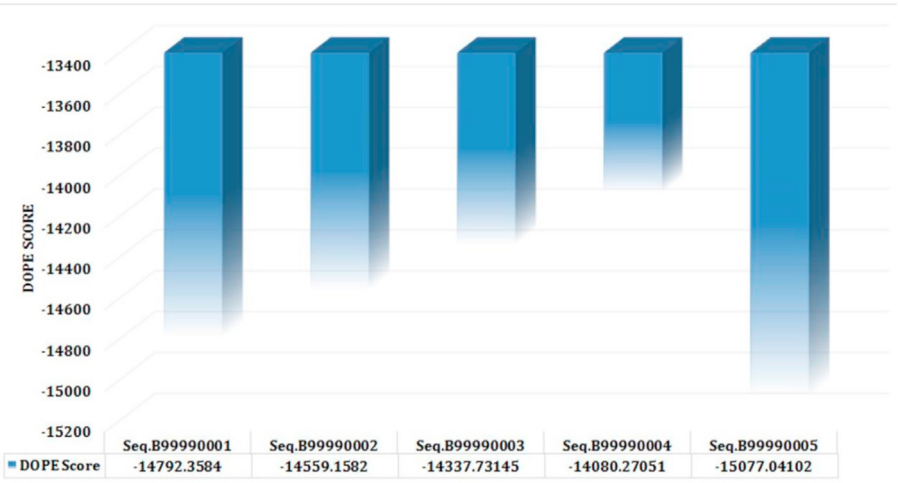

Figure 4. Graphical representation of DOPE score of generated models.

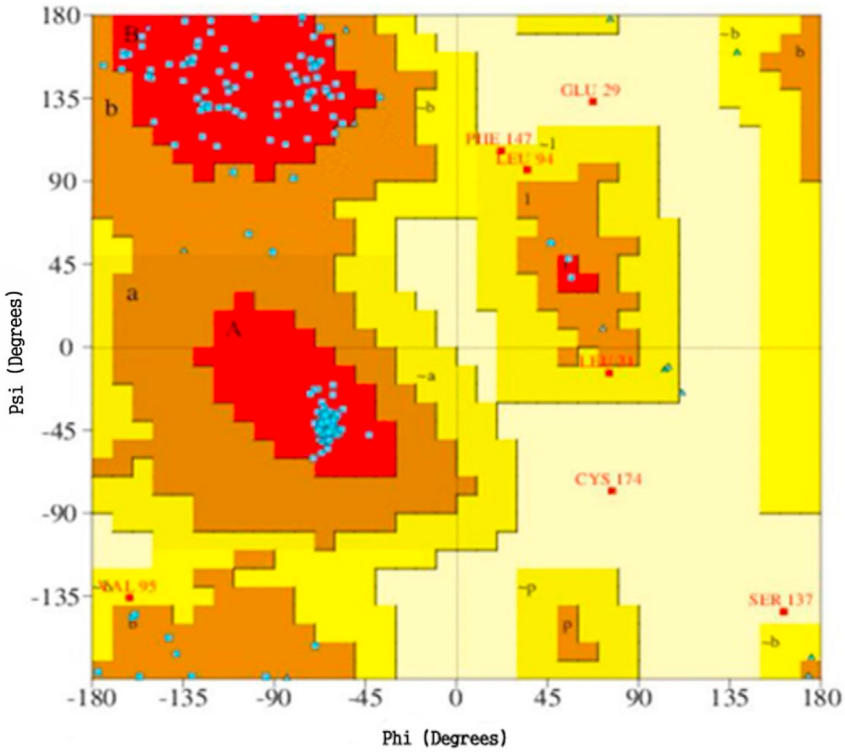

Figure 5. Ramachandran Plot statistics of best model (Seq.B99990002).

3. Results

3.1. Prediction of PSFL protein and their validation

PSFL protein was modelled and selected on the basis of DOPE (Discrete Optimized Protein Energy) score and Ramachandran plot statistics (Table 2) (Figures 4, 5, and 6). According to Ramachandran Plot statistics, the second model of presenilin stabilization factor-like protein [*Homo sapiens*] had 84.7% most favourable region which was the highest among the five models generated. Best model structure showed properties like 84.7% in most favoured regions containing 138 AA residues, 11.0% additional allowed regions containing 18 AA residues, 2.5% generously allowed regions containing 4 AA residues, 1.8% disallowed regions containing 3 AA residues [Table 1]. Finally, Seq.B99990002 was selected as the best PSFL Protein model on the basis of PROCHECK Statistics for docking (Table 2).

3.2. Analysis of binding affinity with PSFL modelled protein and ligand database

802 ligands from database were screened and selected on the basis of binding affinity (kcal/mol). Top 10 ligands in the range were Casuarictin, Saponins, Tellimagrandin II, Digalloyl glucose, Phlorotannin, Carissic acid, Enoxolone, Tigogenin, Astilbin, 18 Alpha-glycyrrhetinic acid having -12.9, -12.3, -11.4, -11.1, -10.8, -10.7, 10.7, -10.6, -10.5, -10.3 binding affinities respectively and were further subjected to molecular

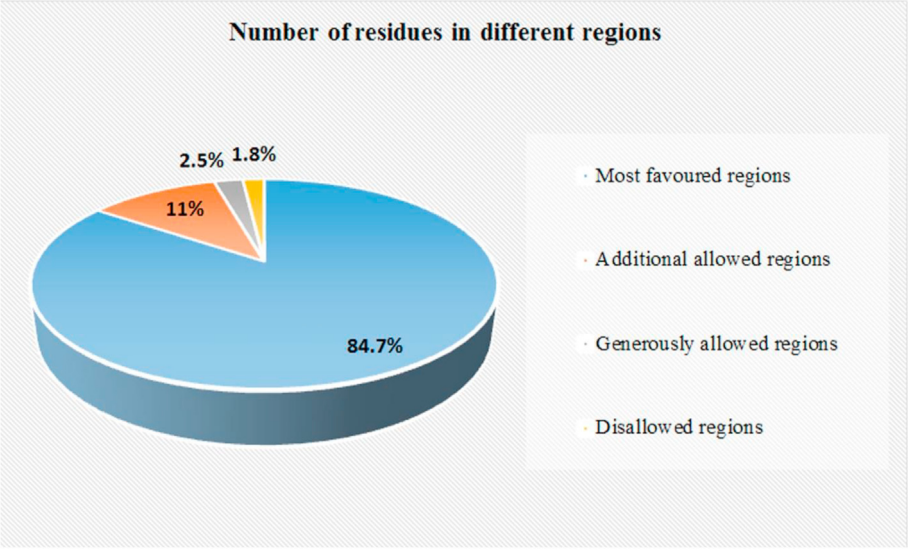

Figure 6. Pie chart depicting Ramachandran plot statistics of predicted structure (Seq.B99990002).

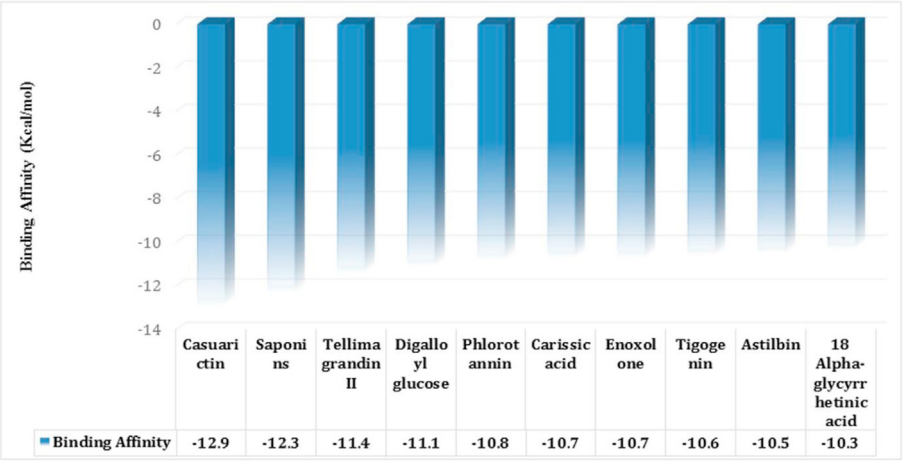

Figure 7. Binding affinity of the best 10 ligands binding with PSFL protein.

Table 3. Binding affinity of the best 10 ligands.

S.No.	Ligands	Binding Affinity
1.	Casuarictin	-12.9
2.	Saponins	-12.3
3.	Tellimagrandin II	-11.4
4.	Digalloyl glucose	-11.1
5.	Phlorotannin	-10.8
6.	Carissic acid	-10.7
7.	Enoxolone	-10.7
8.	Tigogenin	-10.6
9.	Astilbin	-10.5
10.	18 Alpha-glycyrrhetinic acid	-10.3

docking [Figure 7] [Table 3]. Three ligands, namely Saponins, Casuarictin, and Enoxolone finally showed the lowest docked energy -16.19, -13.39, and -9.33, respectively [Figure 8] [Tables 4 and 5]. Saponins, Casuarictin and Enoxolone could be used as a potential inhibitor of PSFL protein. For validation of binding affinity and docked energy of the top three best protein ligands complex, Molecular dynamics simulation was performed. Hydrophobic interactions, hydrogen bonds, and π-stacking were observed in the ligand-protein complex [Figure 9(a-c)]. Interacting residues are shown in Tables 6a-b, 7a-c and 8a-b. Interaction between ligand and protein was analyzed by using Protein-Ligand Interaction Profiler (PLIP) tool [46].

3.3. Analysis of stability of ligand-protein complex

Based on the lowest docked energy, three complexes (Saponin-PSFL complex, Casuarictin-PSFL complex, and Enoxolone-PSFL Complex) were

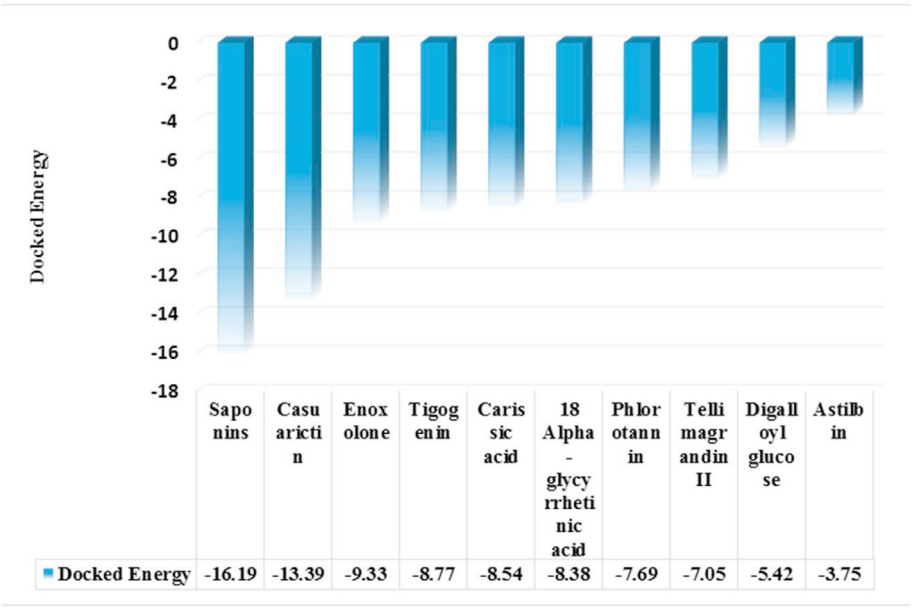

Figure 8. Bar graph representation of docked energy of the best 10 ligands.

Table 4. Docked energy of top 10 ligands against PSFL protein.

S.No.	Ligands	Docked Energy
1.	Saponins	-16.19
2.	Casuarictin	-13.39
3.	Enoxolone	-9.33
4.	Tigogenin	-8.77
5.	Carissic acid	-8.54
6.	18 Alpha-glycyrrhetinic acid	-8.38
7.	Phlorotannin	-7.69
8.	Tellimagrandin II	-7.05
9.	Digalloyl glucose	-5.42
10.	Astilbin	-3.75

Table 5. Entry ID, docked energy and interacting residues of finally selected ligands.

Ligand's name	Entry ID	Docked Energy	Interacting residues
Saponins	Structure2D_CID_21630000	-16.19	PRO73A,PHE107A,ASP109A,SER33A,ILE34A,SER42A,ILE56A,SER58A,ASP81A
Casuarictin	Structure2D_CID_73644	-13.39	ASP81A,PHE108A,LEU46A,LEU71A,SER82A,VAL106A,GLU112A,PHE108A
Enoxolone	zinc_19203131	-9.33	LEU46A,ASP81A,PHE107A,PHE108A,GLU112A,VAL106A

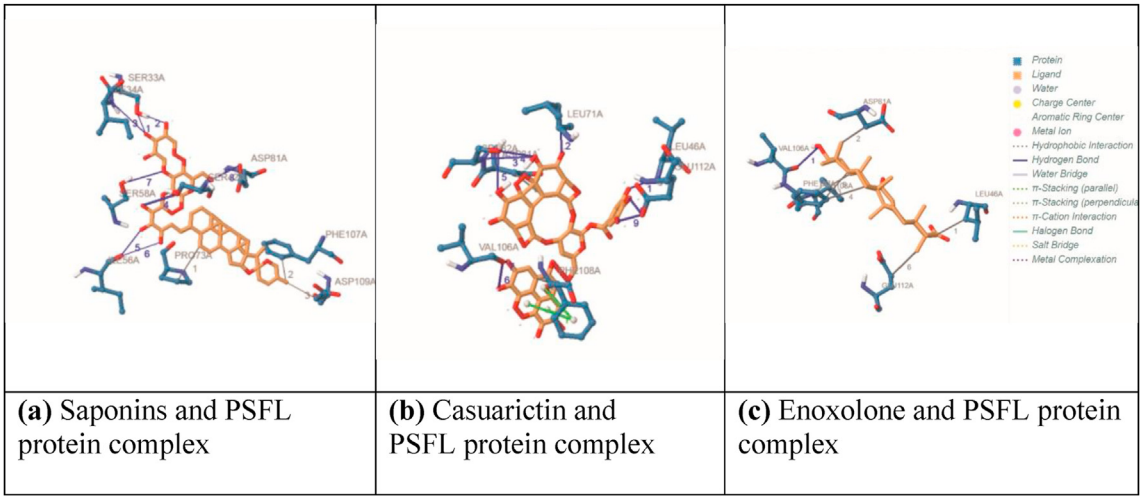

(a) Saponins and PSFL protein complex | **(b)** Casuarictin and PSFL protein complex | **(c)** Enoxolone and PSFL protein complex

Figure 9. Representation of interacting residues (a) Saponins and PSFL protein complex, (b) Casuarictin and PSFL protein complex, (c) Enoxolone and PSFL protein complex.

Table 6. Hydrophobic Interactions and Hydrogen bonds between Saponin and PSFL protein. Orange dashed line show hydrophobic interactions and blue line show hydrogen bonds.

(a) Hydrophobic Interactions

Index	Residue	AA	Distance	Ligand Atom	Protein Atom
1	73A	PRO	3.63	1801	678
2	107A	PHE	3.82	1809	992
3	109A	ASP	3.27	1809	1013

(b) Hydrogen Bonds

Index	Residue	AA	Distance H-A	Distance D-A	Donor Angle	Protein donor?	Side chain	Donor Atom	Acceptor Atom
1	33A	SER	2.19	2.60	126.00	✗	✓	1781 [O2]	335 [O3]
2	33A	SER	1.90	2.83	163.89	✓	✓	335 [O3]	1782 [O2]
3	34A	ILE	3.11	3.97	142.65	✓	✗	339 [Nam]	1781 [O2]
4	42A	SER	2.87	3.58	132.41	✓	✓	407 [O3]	1777 [O2]
5	56A	ILE	3.33	3.69	121.21	✗	✗	1778 [O2]	535 [O2]
6	56A	ILE	3.55	3.97	129.57	✗	✗	1780 [O2]	535 [O2]
7	58A	SER	3.03	3.94	160.68	✓	✓	549 [O3]	1772 [O2]
8	81A	ASP	2.46	3.07	169.45	✗	✓	1775 [O3]	740 [O3]

Table 7. Hydrophobic Interactions, Hydrogen bonds and π-Stacking between Casuarictin and PSFL protein complex. Orange dashed line show hydrophobic interactions, blue line show hydrogen bonds, and green line show π-Stacking.

(a) Hydrophobic Interactions

Index	Residue	AA	Distance	Ligand Atom	Protein Atom
1	81A	ASP	3.74	1795	738
2	108A	PHE	3.49	1793	1001

(b) Hydrogen Bonds

Index	Residue	AA	Distance H-A	Distance D-A	Donor Angle	Protein donor?	Side chain	Donor Atom	Acceptor Atom
1	46A	LEU	2.95	3.49	114.41	✓	✗	446 [Nam]	1835 [O3]
2	71A	LEU	2.33	2.93	165.98	✗	✗	1837 [O2]	668 [O2]
3	82A	SER	3.69	4.02	101.95	✓	✗	744 [Nam]	1781 [O2]
4	82A	SER	2.49	2.93	105.04	✗	✓	1781 [O2]	748 [O3]
5	82A	SER	2.52	2.99	107.06	✗	✓	1780 [O2]	748 [O3]
6	106A	VAL	3.09	3.49	126.18	✗	✗	1845 [O2]	985 [O2]
7	106A	VAL	2.15	2.77	176.03	✗	✗	1841 [O2]	985 [O2]
8	112A	GLU	3.36	3.58	106.59	✗	✓	1833 [O3]	1038 [O3]
9	112A	GLU	2.92	3.29	121.11	✗	✓	1831 [O3]	1038 [O3]

(c) π-Stacking

Index	Residue	AA	Distance	Angle	Offset	Type	Ligand Atoms
1	108A	PHE	4.05	29.67	0.24	P	1798, 1799, 1807, 1810, 1814, 1815
2	108A	PHE	4.35	29.66	1.61	P	1793, 1796, 1797, 1798, 1799, 1789
3	108A	PHE	4.45	29.66	1.85	P	1797, 1799, 1805, 1807, 1778, 1779

selected for MD simulation. The RMSD for the Saponins-PSFL complex was found to be approximately 1.22 nm. Saponins-PSFL complex maintained overall stability throughout 20,000 ps of simulation, Enoxolone-PSFL Complex was found to be approximately 1.7 nm, and it showed a gradual increase after ~7000 ps. Casuarictin-PSFL complex was found to be approximately 0.9 nm, and it showed a gradual increase after ~9000ps. Saponins-PSFL complex showed relatively more stability in comparison to Casuarictin-PSFL complex and Enoxolone-PSFL Complex [Figure 10a].

The Rg was also calculated for the Saponins-PSFL complex, Casuarictin-PSFL complex and Enoxolone-PSFL complex to assess the compactness of the complex structure. The Rg range of the Saponins-PSFL complex structure is between 2.1nm and 2.4 nm. From 0 to ~1000 ps, there is a continuous increase in the Rg value from 2.2 nm to 2.4 nm and further decrease till 2500 ps. After that, it showed stability till 20000 ps. Rg range of Casuarictin-PSFL complex structure is between 1.9 nm and 2.4 nm. From 0 to ~1000 ps, there is a continuous increase in the Rg value from 2.2 nm to 2.4 nm and further decreased and showed stability between 7000ps to 12000 ps and between 15000ps to 20000ps. Rg range of Enoxolone-PSFL Complex structure is between 1.85 nm to 2.25 nm. From 0 ps to 400ps, there is a gradual decrease from 2.2 nm to 2.02 nm and further increase upto 1000ps. It showed stability between 10000ps to 20000ps [Figure 10b].

The SASA was also calculated for Saponins-PSFL complex, Casuarictin-PSFL complex and Enoxolone-PSFL Complex. The SASA range of Saponins-PSFL complex structure lies between 111 and 118 nm^2. The resulting Saponins-PSFL complex showed an increase in the SASA at ~2000 ps and then decreased till 8000 ps and then maintained stability till 20000 ps. Casuarictin-PSFL complex structure lies between 106 and 116 nm^2. The resulting Casuarictin-PSFL complex showed a gradual decrease in the SASA from 0 to ~5000 ps and then stable till 20000ps. Enoxolone-PSFL Complex structure lies between 107.5 nm^2 and 120 nm^2

Table 8. Hydrophobic Interactions and Hydrogen bonds between Enoxolone and PSFL protein complex. Orange dashed line show hydrophobic interactions and blue line show hydrogen bonds.

(a) Hydrophobic Interactions

Index	Residue	AA	Distance	Ligand Atom	Protein Atom
1	46A	LEU	3.32	1770	449
2	81A	ASP	3.59	1794	738
3	107A	PHE	3.97	1784	992
4	107A	PHE	3.69	1786	994
5	108A	PHE	3.43	1780	1001
6	112A	GLU	3.35	1796	1035

(b) Hydrogen Bonds

Index	Residue	AA	Distance H-A	Distance D-A	Donor Angle	Protein donor?	Side chain	Donor Atom	Acceptor Atom
1	106A	VAL	2.37	2.82	107.26	✖	✖	1800 [O3]	985 [O2]

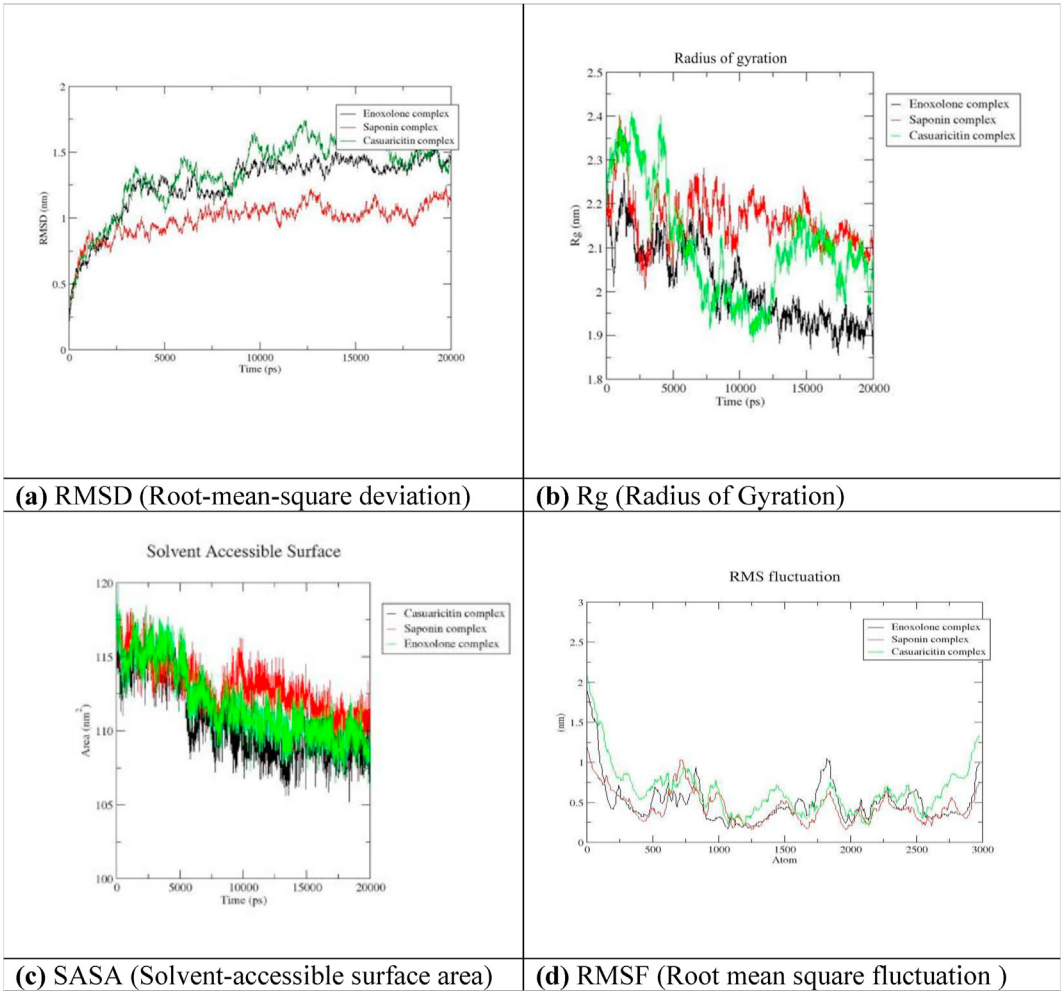

Figure 10. Molecular dynamics (MD) simulation results. (a) RMSD (Root-mean-square deviation), (b) Rg (Radius of Gyration), (c) SASA (Solvent-accessible surface area), (d) RMSF (Root mean square fluctuation).

and showed fluctuation till 8000ps and then maintained stability till 20000ps [Figure 10c].

The RMSF for Saponins-PSFL complex was found to be approximately 0.75 nm. Saponins-PSFL complex maintained overall stability throughout 3000 atoms. Enoxolone-PSFL Complex was found to be approximate 0.8 nm, and it showed a gradual decrease from 0 to 250 atoms, and then it maintained stability until 3000 atoms. Casuarictin-PSFL complex was found to be approximately 0.85 nm, and it showed a gradual decrease after 0 to ~500 atoms and further maintained stability until 2500 atoms. Saponins-PSFL complex showed more stability in comparison to Casuarictin-PSFL complex and Enoxolone-PSFL Complex [Figure 10d].

4. Discussion

Currently, there is no target specific treatment for AD. Available drugs only suppress the symptoms and can only temporarily slow down the progression of AD. Suppression of symptoms leaves limited

improvements in the quality of life for AD patients. So, there is a worldwide effort in progress to find the best possible way to treat AD completely, delay the onset of disease, and prevent it from developing. Finding a potent inhibitor of PSFL protein to treat AD may be considered as a rising hope.

In this study Casuarictin, Saponins, and Enoxolone emerged as promising herbal therapeutics against Alzheimer's disease. Thus, these three phytochemicals may be selected as the ligands for targeting protein PSFL. Though trajectory, RMSD, RMSF, Rg, and SASA analysis confirmed the docking results and it was observed that Saponin-PSFL complex had the highest stability scores, but saponins are toxic compounds and thus may possess limited scope to qualify as drug molecules. Casuarictin is an ellagitannin, which is hydrolysable form of tannin. Casuarictin is generally found in Casuarina and Stachyurus species. While Enoxolone is a pentacyclic triterpenoid first reported from the herb liquorice. It is a derivative of the beta-amyrin and is used for its expectorant, antifungal, and antibacterial properties. Amongst the three molecules, Casuarictin seems to have the highest potential for further research and analysis as therapeutic agent of Alzheimer's disease. These findings will facilitate identification of herbal compounds as inhibitors of PSFL protein to suppress amyloid β protein production and thus provide a potential alternative for treatment of Alzheimer's disease.

Declarations

Author contribution statement

A. Mani: Conceived and designed the experiments; Contributed reagents, materials, analysis tools or data; Wrote the paper.

R. Kumari and A. Chaudhary: Analyzed and interpreted the data; Contributed reagents, materials, analysis tools or data; Wrote the paper.

Funding statement

This work was supported by SERB New Delhi (CRG/2018/001912).

Declaration of interests statement

The authors declare no conflict of interest.

Additional information

No additional information is available for this paper.

References

[1] H.J. Möller, M.B. Graeber, The case described by Alois Alzheimer in 1911. Historical and conceptual perspectives based on the clinical record and neurohistological sections, Eur. Arch. Psychiatr. Clin. Neurosci. 248 (1998) 111–122.

[2] A. Chaudhary, P.K. Maurya, B.S. Yadav, S. Singh, A. Mani, Current therapeutic targets for alzheimer's disease, J. Biomed. 3 (2018) 74–84.

[3] D.J. Selkoe, Amyloid β protein precursor and the pathogenesis of Alzheimer's disease, Cell 58 (1989) 611–612.

[4] S.E. Arnold, B.T. Hyman, J. Flory, A.R. Damasio, G.W. Van Hoesen, The topographical and neuroanatomical distribution of neurofibrillary tangles and neuritic plaques in the cerebral cortex of patients with alzheimer's disease, Cerebr. Cortex 1 (1991) 103–116.

[5] J. Hardy, D.J. Selkoe, The amyloid hypothesis of Alzheimer's disease: progress and problems on the road to therapeutics, Science 297 (2002) 353–356.

[6] T.D. Bird, Alzheimer Disease Overview, 1993. http://www.ncbi.nlm.nih.gov/pubmed/20301340. (Accessed 16 January 2020).

[7] T.G. Beach, The history of alzheimer's disease: three debates, J. Hist. Med. Allied Sci. 42 (1987) 327–349.

[8] P. Eikelenboom, E. van Exel, J.J.M. Hoozemans, R. Veerhuis, A.J.M. Rozemuller, W.A. van Gool, Neuroinflammation – an early event in both the history and pathogenesis of alzheimer's disease, Neurodegener. Dis. 7 (2010) 38–41.

[9] E. Karran, M. Mercken, B. De Strooper, The amyloid cascade hypothesis for Alzheimer's disease: an appraisal for the development of therapeutics, Nat. Rev. Drug Discov. 10 (2011) 698–712.

[10] D. Scheuner, C. Eckman, M. Jensen, X. Song, M. Citron, N. Suzuki, T.D. Bird, J. Hardy, M. Hutton, W. Kukull, E. Larson, E. Levy-Lahad, M. Viitanen, E. Peskind, P. Poorkaj, G. Schellenberg, R. Tanzi, W. Wasco, L. Lannfelt, D. Selkoe, S. Younkin, Secreted amyloid β-protein similar to that in the senile plaques of Alzheimer's disease is increased in vivo by the presenilin 1 and 2 and APP mutations linked to familial Alzheimer's disease, Nat. Med. 2 (1996) 864–870.

[11] A.A. Rao, K. Kumar Reddi, H. Thota, A.A. Rao, Bioinformatic analysis of alzheimer's disease using functional protein sequences, J. Proteomics Bioinformatics-Open Access Res. Artic. JPB. 1 (2008).

[12] I. Bezprozvanny, M.P. Mattson, Neuronal calcium mishandling and the pathogenesis of Alzheimer's disease, Trends Neurosci. 31 (2008) 454–463.

[13] B. De Strooper, P. Saftig, K. Craessaerts, H. Vanderstichele, G. Guhde, W. Annaert, K. Von Figura, F. Van Leuven, Deficiency of presenilin-1 inhibits the normal cleavage of amyloid precursor protein, Nature 391 (1998) 387–390.

[14] M. Citron, D. Westaway, W. Xia, G. Carlson, T. Diehl, G. Levesque, K. Johnson-Wood, M. Lee, P. Seubert, A. Davis, D. Kholodenko, R. Motter, R. Sherrington, B. Perry, H. Yao, R. Strome, I. Lieberburg, J. Rommens, S. Kim, D. Schenk, P. Fraser, P. St, Hyslop George, D.J. Selkoe, Mutant presenilins of Alzheimer's disease increase production of 42-residue amyloid β-protein in both transfected cells and transgenic mice, Nat. Med. 3 (1997) 67–72.

[15] J. Hardy, Amyloid, the presenilins and Alzheimer's disease, Trends Neurosci. 20 (1997) 154–159.

[16] C. Haass, B. De Strooper, The presenilins in Alzheimer's disease - proteolysis holds the key, Science 286 (1999) 916–919.

[17] A. Zhou, J. Hu, L. Wang, G. Zhong, J. Pan, Z. Wu, A. Hui, Combined 3D-QSAR, molecular docking, and molecular dynamics study of tacrine derivatives as potential acetylcholinesterase (AChE) inhibitors of Alzheimer's disease, J. Mol. Model. 21 (2015) 1–12.

[18] J. Hardy, M. Hutton, The genes involved in alzheimer's disease, in: Alzheimer's Dis., Springer Berlin Heidelberg, 1996, pp. 49–59.

[19] Alzheimer's Association, 2018 Alzheimer's Disease Facts And Figures Includes a Special Report on the Financial and Personal Benefits of Early Diagnosis, 2018.

[20] Alzheimer's facts and figures report, alzheimer's association (n.d.), https://www.alz.org/alzheimers-dementia/facts-figures. (Accessed 31 December 2019).

[21] M. Sahoo, L. Jena, S. Daf, S. Kumar, Virtual screening for potential inhibitors of NS3 protein of zika virus, Genomics Inform 14 (2016) 104.

[22] F.A. Larik, A. Saeed, P.A. Channar, U. Muqadar, Q. Abbas, M. Hassan, S.Y. Seo, M. Bolte, Design, synthesis, kinetic mechanism and molecular docking studies of novel 1-pentanoyl-3-arylthioureas as inhibitors of mushroom tyrosinase and free radical scavengers, Eur. J. Med. Chem. 141 (2017) 273–281.

[23] G. Kumar, R. Patnaik, Exploring neuroprotective potential of Withania somnifera phytochemicals by inhibition of GluN2B-containing NMDA receptors: an in silico study, Med. Hypotheses 92 (2016) 35–43.

[24] J.A. Joseph, B. Shukitt-Hale, N.A. Denisova, D. Bielinski, A. Martin, J.J. McEwen, P.C. Bickford, Reversals of age-related declines in neuronal signal transduction, cognitive, and motor behavioral deficits with blueberry, spinach, or strawberry dietary supplementation, J. Neurosci. 19 (1999) 8114–8121.

[25] A.J. Hampson, M. Grimaldi, J. Axelrod, D. Wink, Cannabidiol and (-)Δ9-tetrahydrocannabinol are neuroprotective antioxidants, Proc. Natl. Acad. Sci. U. S. A. 95 (1998) 8268–8273.

[26] S.Y. Park, D.S.H.L. Kim, Discovery of natural products from Curcuma longa that protect cells from beta-amyloid insult: a drug discovery effort against Alzheimer's disease, J. Nat. Prod. 65 (2002) 1227–1231.

[27] M.M. Essa, R.K. Vijayan, G. Castellano-Gonzalez, M.A. Memon, N. Braidy, G.J. Guillemin, Neuroprotective effect of natural products against Alzheimer's disease, Neurochem. Res. 37 (2012) 1829–1842.

[28] S. Dallakyan, A.J. Olson, Small-molecule library screening by docking with PyRx, Methods Mol. Biol. 1263 (2015) 243–250.

[29] Presenilin stabilization factor-like protein [Homo sapiens] - protein - NCBI (n.d.), https://www.ncbi.nlm.nih.gov/protein/AAN63817.1. (Accessed 10 October 2020).

[30] B. Webb, A. Sali, Comparative protein structure modeling using MODELLER, Curr. Protoc. Bioinforma. 54 (2016), 5.6.1-5.6.37.

[31] S.F. Altschul, T.L. Madden, A.A. Schäffer, J. Zhang, Z. Zhang, W. Miller, D.J. Lipman, Gapped BLAST and PSI-BLAST: a new generation of protein database search programs, Nucleic Acids Res. 25 (1997) 3389–3402.

[32] R.W.W. Hooft, C. Sander, G. Vriend, Objectively judging the quality of a protein structure from a ramachandran plot, Bioinformatics 13 (1997) 425–430.

[33] E. Lionta, G. Spyrou, D. Vassilatis, Z. Cournia, Structure-Based virtual screening for drug discovery: principles, applications and recent advances, Curr. Top. Med. Chem. 14 (2014) 1923–1938.

[34] X.-Y. Meng, H.-X. Zhang, M. Mezei, M. Cui, Molecular docking: a powerful approach for structure-based drug discovery, Curr. Comput. Aided Drug Des. 7 (2011) 146–157.

[35] D. Vanaja, K. Yellamma, Molecular docking studies on evolvulus alsinoides compounds against TAU protein in alzheimer's disease, Bioinformatics 3 (2014).

[36] C. Selvaraj, S. Sakkiah, W. Tong, H. Hong, Molecular dynamics simulations and applications in computational toxicology and nanotoxicology, Food Chem. Toxicol. 112 (2018) 495–506.
[37] S. Sakkiah, R. Kusko, W. Tong, H. Hong, Applications of molecular dynamics simulations in computational toxicology, in: Challenges Adv. Comput. Chem. Phys., Springer, 2019, pp. 181–212.
[38] M. Karplus, J.A. McCammon, Molecular dynamics simulations of biomolecules, Nat. Struct. Biol. 9 (2002) 646–652.
[39] D. Van Der Spoel, E. Lindahl, B. Hess, G. Groenhof, A.E. Mark, H.J.C. Berendsen, GROMACS: fast, flexible, and free, J. Comput. Chem. 26 (2005) 1701–1718.
[40] A. Cordomí, G. Caltabiano, L. Pardo, Membrane protein simulations using AMBER force field and Berger lipid parameters, J. Chem. Theor. Comput. 8 (2012) 948–958.
[41] S.P. Hirshman, J.C. Whitson, Steepest-descent moment method for three-dimensional magnetohydrodynamic equilibria, Phys. Fluids 26 (1983) 3553–3568.
[42] T.E. Cheatham, J.L. Miller, T. Fox, T.A. Darden, P.A. Kollman, Molecular dynamics simulations on solvated biomolecular systems: the particle mesh Ewald method leads to stable trajectories of DNA, RNA, and proteins, J. Am. Chem. Soc. 117 (1995) 4193–4194.
[43] B. Hess, H. Bekker, H.J.C. Berendsen, J.G.E.M. Fraaije, LINCS: a linear constraint solver for molecular simulations, J. Comput. Chem. 18 (1997) 1463–1472.
[44] E. Lindahl, B. Hess, D. van der Spoel, GROMACS 3.0: a package for molecular simulation and trajectory analysis, J. Mol. Model. 7 (2001) 306–317.
[45] P.J. Turner, XMGRACE, version 5.1. 19, Cent. Coast. Land-Margin Res. Oregon Grad. Inst. Sci. Technol. Beaverton, OR. (2005).
[46] S. Salentin, S. Schreiber, V.J. Haupt, M.F. Adasme, M. Schroeder, PLIP: fully automated protein-ligand interaction profiler, Nucleic Acids Res. 43 (2015) W443–W447.